國立臺灣大學高分子科學與工程學研究所

碩士論文

Graduate Institute of Polymer Science and Engineering
College of Engineering
National Taiwan University

Master Thesis

聚 4-乙烯基吡啶與 3,5-雙(十六烷氧基)苯甲酸形成之超分子的相分離行為與結構分析

Phase Behaviors and Structure of Supramolecules Formed by Poly(4-vinylpyridine) and 3,5-Bis(hexadecyloxyl)benzoic Acid

許仲儉

Chung-Chien Hsu

指導教授：童世煌 博士

Advisor: Shih-Huang Tung, Ph.D.

中華民國 104 年 8 月

August, 2015

誌謝

感謝老師、同學以及我的家人對我的任性一直以來的容忍。非常感謝，也非常抱歉，抱歉讓你們失望，以及給你們添了許多的麻煩。另外也要感謝精神科的那位醫生，儘管利他能效用不大，但至少讓我有個可以宣洩壓力的對象。

感謝大家，珍重再見。

中文摘要

在本研究中探討了由聚 4-乙烯基吡啶(Poly(4-vinylpyridine), P4VP)與 3,5-雙(十六烷氧基)苯甲酸(3,5-Bis(hexadecyloxyl)benzoic acid, BHBA)經由氫鍵結合而成的超分子複合體。藉由傅立葉轉換紅外光譜觀察了在超分子複合體中的 P4VP 與 BHBA，或著自由 BHBA 二聚體間的氫鍵接合情形。另外也利用了小角度 X 光繞射(Small angle X-ray scattering, SAXS)與廣角度 X 光繞射(Wide angle X-ray scattering, WAXS) 來了解超分子複合體和過剩的 BHBA 分子的結構型態，以及藉由示差掃描熱分析儀(Differential scanning calorimetry, DSC)與變溫 SAXS 觀察其熱性質與隨溫度的形態變化。由於其本身的雙尾分子結構，純的 BHBA 在退火及淬火後，分別產生了特殊的結晶結構以及層狀結構，並也在之後的 P4VP(BHBA)$_x$ 複合體中出現。另外意外地發現儘管超分子複合體有生成，在 SAXS 的散射中並未觀察到有生成任何規整結構，經推測原因應是 BHBA 的尾部結構的立體障礙對於形成層狀結構而言過大，而對於六角堆積柱狀結構則又過小。隨著 BHBA 的增加，在經過一飽和的平緩區後，在 FTIR 中亦可觀察到側鏈的脫落，而且因側鏈脫落造成的 P4VP 蜷曲也可由 SAXS 確定。在 P4VP(BHBA)$_x$，且 x 是 BHBA 對 4VP 重複單元的比例的情況下，在 $x = 0.8$ 時觀察到有特殊的現象。在 $x = 0.8$ 時，BHBA 應已有剩餘，但卻未能形成羧酸二聚體，而且超分子複合體的排列特別地不規整。這些結果被解釋為因為剩餘的BHBA量不足以形成聚集，並穿插在超分子複合體的BHBA部分，進而干擾了 BHBA 層間的交互穿插。對於雙尾的側鏈分子而言，這是一個不同於其他單尾或三尾的側鏈分子的獨有的特徵。

關鍵字：氫鍵、超分子、雙尾介面活性劑

ABSTRACT

In this study, the supramolecular complex of 3,5-bis(hexadecyloxyl)benzoic acid (BHBA) and Poly(4-vinylpyridine) (P4VP) via hydrogen bonding is investigated. FTIR was utilized for observing the hydrogen bonding between P4VP and BHBA or in free BHBA dimers. SAXS and WAXS was applied for studying the morphology of supramolecular complex and excess BHBA molecules, and the thermal property and morphology evolution with temperature is studied by DSC and in situ SAXS and WAXS. Due to its two-tailed molecular structure, pristine BHBA forms unique crystalline structure after annealed and lamellar structure after quenched, which both found in P4VP(BHBA)$_x$ complexes. Surprisingly, though with formation of supramolecular complex, no ordered structure is found in SAXS profile. The reason is considered as that the steric hindrance of tails of BHBA is too large for lamellar structure, and too weak for hexagonally-packing cylindrical structure. With addition of BHBA, detachment of side chains due to crystallizing competition is observed by FTIR after a saturating plateau and coiling of P4VP due to detachment is also confirmed by SAXS. For P4VP(BHBA)$_x$, where x is the molar ratio of BHBA to 4VP repeating unit, it is found the x = 0.8 is unique point where BHBA is shown excess but does not form carboxylic acid dimer, and the alignment of supramolecular complex is especially less ordered. This is possibly because the amount of excess BHBA is too little for self-aggregating and they insert in BHBA domain in supramolecular complex, thus interfering with the interdigitating between BHBA domains. This is the distinct characteristic of supramolecular complex with two-tailed side chain molecule different from the complexes with single or three-tailed ones.

Key word: hydrogen bonding; supramolecules; two-tailed surfactant

CONTENTS

LIST OF FIGURES

Chapter 1 Introduction

Supramolecule chemistry, which can be identified as “association of multiple chemical species held together by intermolecular forces,” is a popular methodology in recent decades, especially in the topic of molecule self-assembling[1]. Within intermolecular forces, hydrogen bond is vastly applied in supramolecular self-assembling because preparing hydrogen bonding-based samples are less laborious than its covalent counterparts, and the thermoreversibility hydrogen bonds is beneficial for equilibration process during self-assembly.[2]

Comb-like supramolecules, which were firstly adopted for liquid-crystalline materials, are the most studied class by far among hydrogen-boned copolymer systems.[3] Two advantages are the reason that hydrogen bonding is widely applied in comb-like architecture building. One is that performance of comb-like supramolecules can be simply controlled by grafting density, which can be adjusted by stoichiometric method, and volume fraction of the nonpolar alkyl tails, which can be modified by selecting grafting surfactant. Another is that unlike electrostatic bond or coordination interaction, hydrogen bond is not too strong and some bonding sites of backbone in polar domains can remain unoccupied with less energetic penalties. This enhance the formation of highly ordered simple structure, e.g. lamella, of hydrogen-boned comb-like supramolecules, comparing with other systems with other intermolecular forces.[2]

Among hydrogen-boned comb-like systems, the system with poly(4-vinylpyridine) (P4VP) backbone is widely studied.[4-14] The system with P4VP backbone and few types of single tail alkyl phenols was investigated by the groups of ten Brinke and Ikkala.[11-14] Without enough steric hindrance of nonpolar domain, P4VP and single tail alkyl phenol systems are mostly ended with lamellar structure unless longer alky tail (> 15 C)

is utilized.[11] On the other hand, by adopting surfactant with thee alkyl tails to increase steric hindrance and volume of nonpolar domain, ordered cylindrical structure can be achieved at high grafting density, while lamellar structure can still be found at low grafting density.[4-10] However it is also reported that at grafting density over saturation detachment of surfactants may occur driven by crystallization of additional surfactants.[4]

Nevertheless, as systems with single-tailed and three-tailed surfactants were studied in detail, the system with two-tailed surfactants is still left untouched. With higher steric hindrance than single-tailed counterparts and more free space than three-tailed ones, supramolecular system with two-tailed surfactants is expected to perform some other interest results, which is the target of this research. For comparison, the two-tailed surfactant used in this research is 3,5-bis(hexadecyloxyl)benzoic acid (BHBA), with better solubility than 3,4-bis(hexadecyloxyl)benzoic acid in pretest and resembling 3,4,5-tris(hexadecyloxyl)benzoic acid (THBA) used by Lai et al. [4] but only with two alkyl tails, and comparison will be done in discussion.

Chapter 2 Literature Reviews

2.1 Hydrogen-Bonded Comb-like Supramolecules

Hydrogen-bonded comb-like supramolecules, which is the most studied class of hydrogen-bonded supramolecule system[3], was originally innovated for introducing mesogenic side chains onto polymer backbone for fabricating liquid-crystalline materials.[2] This methodology was than adopted for building supramolecular analogies of comb-like covalent copolymers, since it is much simpler for obtaining desired architecture by simply incorporating desired side chain molecules without the need of laborious covalent synthesis.[15, 16] Therefore, such methodology has been introduced for building specific structures, such as hexagonally-packing cylinders, and applied in manufacturing various functional materials or advanced hierarchical structures.[16-19]

The effect of introduced side chain molecules has been systemically investigated by ten Brinke and Ikkala.[11-14, 20] Proton donating group on side chain molecules was reported as that phenolic group performs better than alcoholic, carboxylic and amino groups[20], though it was later found by Wang et al. that benzoic group performs stronger hydrogen bonding and becomes another option.[5] The methodology by utilizing FTIR for quantifying side chain grafting density was also established.[21] Direct image of lamellar structure formed by supramolecules was also captured by transmission electron microscopy (TEM).[14] Above mentioned researches provide a complete schema for studying supramolecules with other types of side chains. However the side chain surfactants ten Brinke and Ikkala adopted are all with single tail only, of which steric hindrance is insufficient for building hexagonally-packing cylinders, unless the tail is long enough (> 15 C).[11]

For solving the problem of insufficient steric hindrance, it is reasonable for amplify

steric hindrance by increasing the number of alkyl tails. It has been many studies achieved hexagonally-packing cylindrical structure by increasing tail number and applied in other applications.[6-10] Wang et al. have systemically studied the effect of utilizing three-tailed surfactant, e.g. 3,4,5-tris(dodecyloxy)benzoic acid (TDBA), which contains three tails shorter than 15 carbons suggested by ten Brinke and Ikkala.[5, 11] It is found that although with shorter tails, hexagonally-packing cylindrical structure is achieved, and the structure will evolve with grafting density, from lamella at low density to hexagonally-packing cylinders at high density, shown as Fig. 2.1. Lai et al. also investigated systems with three-tailed surfactant by applying 3,4,5-tris(hexadecyloxy)benzoic acid (THBA) with longer tails, and found that although lamellar and hexagonally-packing cylinders still perform at low and medium molar ratio of THBA, side chains dissociate from P4VP at high molar ratio after the saturation. Dissociation during heating process and following recrystallization into free crystals are also observed by DSC. It is considered that the intermolecular interaction energy of long tails is strong enough for overcoming hydrogen bonding energy. Therefore at the circumstance that there are free THBA molecules for crystallization or hydrogen bond is weakened by heating, the dissociation occurs due to the competition between intermolecular interaction energy of long tails and hydrogen bonding energy.[4]

Though hydrogen-bonded comb-like supramolecular system with various side chain molecules has been studied in detail, system with two-tailed side chain molecules is remained unknown. With steric hindrance higher than single-tailed surfactant and intermolecular interaction less than three-tailed one, the system with two-tailed surfactant is expected to perform different than two others.

In this study, 3,5-bis(hexadecyloxyl)benzoic acid (BHBA) is selected as the two-tailed surfactant for comparison with Lai's study with the same length of surfactant carbon

chain tails. Another possible two-tailed surfactant, 3,4-bis(hexadecyloxyl)benzoic acid, was also applied in prior test but due to its poor solubility in chloroform or other solvents, it was excluded from further study.

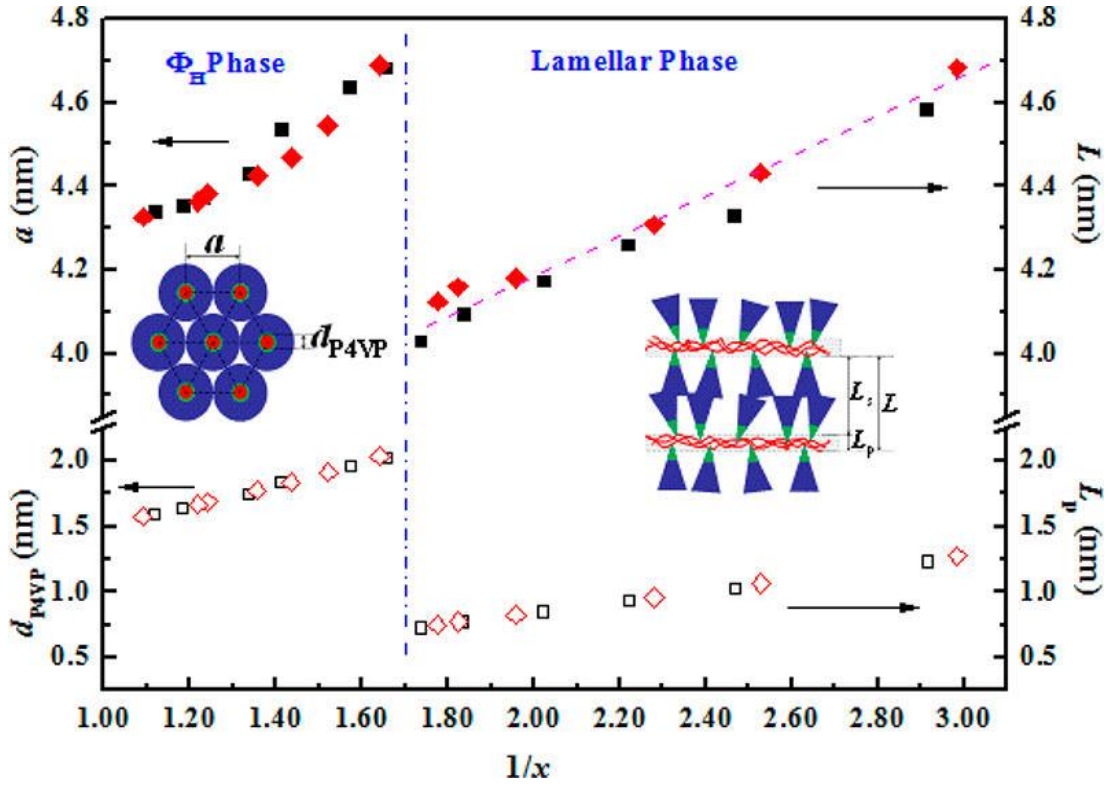

Figure. 2.1 Phase behavior of hydrogen-bonded P4VP and 3,4,5-tris(dodecyloxy)benzoic acid (TDBA) complex with lamellar-to-cylindrical phase transition, where x is the molar ratio of TDBA to 4VP repeating units. Black and red symbols are complexes with molecular weights of P4VP as 82000 g/mol and 19000 g/mol respectively. The dashed pink line is the linear fit of the long period L of lamellar phase, of which the intercept of 3.2 nm is the surfactant layer thickness L_s.[5]

Chapter 3 Experimental Section

3.1 Materials

Poly(4-vinylpyridine) (P4VP, M_n = 15000 g/mol, PDI = 1.25) was bought from Polymer Source, Inc. Chloroform ($CHCl_3$, ≥ 99.8%) was purchased from Avantor Performance Materials, Inc. and used as received. 3,5-Bis(hexadecyloxyl)benzoic acid (BHBA) was generously provided by Prof. Kwang-Ming Lee and his team

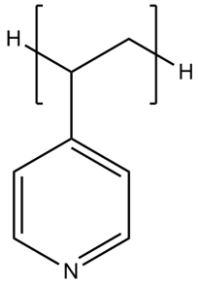

Poly(4-vinylpyridine) (P4VP)

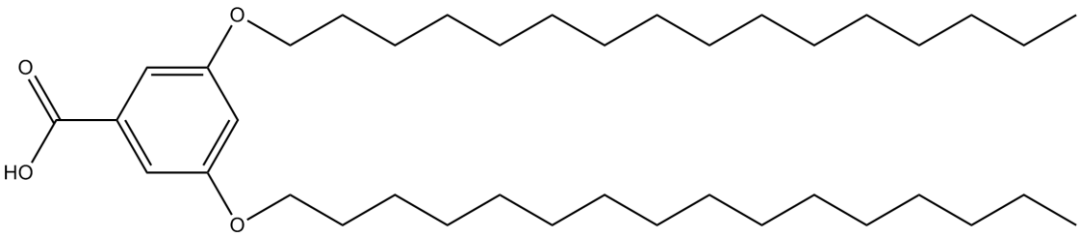

3,5-Bis(hexadecyloxyl)benzoic acid (BHBA)

3.1.1 Sample Preparation

The method was adopted from Lai et al.[4] P4VP was dried in vacuum at 100℃ overnight before used in sample preparing. The designed amount of P4VP and BHBA were dissolved in $CHCl_3$ separately to reach ~ 3 wt%. Then P4VP solution was added into BHBA solution drop by drop and then stirred for over 2 days at ~ 40 ℃ before further experiments. Solid sample was prepared by evaporation of mixture of P4VP-BHBA solution in a Teflon beaker and followed by a thermal annealing at 85℃ in nitrogen for over 5 hours. At the end of annealing, sample was cooled to ambient temperature slowly

for hours. Samples are donated as P4VP(BHBA)$_x$, where x is the molar ratio of BHBA to 4VP repeat units.

3.2 Instruments

3.2.1 Fourier Transform Infrared Spectroscopy (FTIR)

FTIR was applied to study the hydrogen bond between BHBA and 4VP repeat units. Measurement was performed on Jasco 4100 FT-IR spectrometer in transition mode at the resolution of 1 cm^{-1} and 16 scans were done for a sample. Sample was prepared by casting P4VP-BHBA solution onto KBr pellet and followed by annealing the same as above mentioned.

3.2.2 Differential Scanning Calorimeter (DSC)

The thermal property of samples was investigated by using TA Instrument DSC Q200. Samples (~ 3 mg) was heated from 40 ℃ to 100 ℃ under nitrogen condition at a ramping rate of 10 ℃/min. Isothermal heating was held after temperature reached 100℃ and a cycle of cooling and heating between 100 ℃ and -40 ℃ was performed subsequently. Some of the mentioned processes were also performed at the rate of 1 ℃/min for further study.

3.2.3 Small-Angle X-ray Scattering (SAXS) and Wide-Angle X-ray Scattering (WAXS)

SAXS and WAXS experiments were done on beamline B23A1 in the National Synchrotron Radiation Research Center (NSRRC), Hsinchu, Taiwan, with a wavelength λ as 0.827 Å or 1.240 Å. SAXS spectra were collected by a Pilatus 1 M detector (169 mm × 179 mm, 981 pixels × 1043 pixels), as 2-D WAXS patterns were collected by a Flat Panel (1043 pixels × 1043 pixels with resolution of 0.5 mm). By circularly averaging the

2-D pattern, 1-D scattering profiles were reported as scattering intensity I versus scattering vector q, where $q = (4\pi/\lambda)\sin(\theta/2)$ and θ is scattering angle.

Chapter 4 Results and Discussion

4.1 Hydrogen Bonding Complex

Formation of hydrogen bonding between P4VP and BHBA can be detected by analyzing the vibration of chemical bonds via FTIR spectra. In the FTIR spectra Figure. 4.1 of P4VP(BHBA)$_x$ samples, the absorption peaks at 1598 and 994 cm^{-1} which correspond with the stretching mode of pyridine group of pristine P4VP, are observed.[11] With addition of BHBA, the above mentioned peaks both shift to higher wavenumber (from 1598 cm^{-1} to 1607 cm^{-1} and from 994 cm^{-1} to 1015 cm^{-1}) due to formation of hydrogen bonding with carboxylic acid group on BHBA.

For *x* not higher than 0.8, the shift peaks grown with *x* increasing, indicating the hydrogen-binding complex formation was following the addition of BHBA. However when *x* comes to 0.9, the shifted peaks at 1607 and 1015 cm^{-1} stop growing and the peak of pristine BHBA at 1613 cm^{-1} starts growing in instead. Also the peak of carbonyl group of BHBA at 1703 cm^{-1} shift to 1693 cm^{-1}. The shift of carbonyl group shows BHBA start forming carboxylic acid dimer[22] and hydrogen bonding does not increase with more BHBA, indicating that BHBA stop binding with P4VP and start to aggregate by itself for *x* higher than 0.8. Then as *x* reaches 1.2, peak at 1015 cm^{-1} starts attenuating obviously, which may indicates the decrease of hydrogen bonding between P4VP and BHBA, while peak at 1607 cm^{-1} is seriously interrupted by the peak of aromatic ring of pristine BHBA at 1613 cm^{-1} and therefore cannot be told whether attenuation occurred or not.

For further understanding the performance of BHBA at high molar ratio, peak fitting is utilized for quantification of the degree of complexing. By fitting peaks around 1600 cm^{-1} by Voigt amplitude function with Peak Fit software, following peaks can be separated: 1596 cm^{-1} and 1613 cm^{-1} for aromatic ring of BHBA, 1598 cm^{-1} for free

pyridine group of P4VP and 1607 cm^{-1} for hydrogen bonded pyridine group of P4VP. After peak separation, the degree of grafting (f_{HB}) can be estimated by following equation:[5, 21, 23]

$$f_{HB} = \frac{A_{1607}}{A_{1607} + \frac{\alpha_{1598}}{\alpha_{1607}} A_{1598}}$$

where A is the peak area and $\alpha_{1598}/\alpha_{1607}$ is the absorption ratio of peak at 1598 and 1607 cm^{-1}, which is assumed as unity. The estimated degrees of grafting are plotted against molar ration of BHBA:4VP (x) as Figure. 4.. In Figure. 4., it can be observed that the degree of grafting ramps up ($x \leq 0.7$), reaches a plateau around 57% ($0.8 \leq x \leq 1.0$) and drops to 40% drastically ($x \geq 1.2$). This can be interpreted as binding, saturating and detaching of BHBA with increasing BHBA contents. The saturated degree of grafting is only 57% and far lower than theoretical maximum 100% (i.e. every 4VP repeating unit is bound by a BHBA). Low degree of grafting may be attributed to the steric hindrance and self-aggregation competition.[4, 5, 24] For the samples in the plateau region ($0.8 \leq x \leq 1.0$), only the sample $x = 0.8$ does not show carbonyl peak shift of carboxylic acid dimer formation in Fig. 4.1. This may suggest that the additional BHBA in the system of $x = 0.8$ is too few for forming acid dimer and further aggregation. This will be proved in following sections by SAXS, WAXS and DSC analysis.

The detachment of BHBA, which is also reported by Lai et al., is considered to be driven by excess BHBA crystal whose lattice energy is strong enough to overcomes the binding energy of hydrogen bonds between P4VP and BHBA[4], while the formation excess BHBA crystal is also proved by shifting of carbonyl absorption peak.[22]

Consequently, the condition of hydrogen bonding can be summarized into three regimes with different x: the first regime for $x \leq 0.7$ in which hydrogen binding is proportional to the amount of BHBA; the second regime for $0.8 \leq x \leq 1.0$ in which the

binding site is saturated and excess BHBA starts aggregating except $x = 0.8$; and the last regime in which BHBA start detaching from P4VP because of the competition from excess BHBA crystallization.

4.2 Structure Analysis of P4VP(BHBA)$_x$

X-ray scattering techniques were applied for investigating the structure of micro-phase separation of P4VP(BHBA)$_x$ samples. Fig. 4.3 is the SAXS and WAXS profile of P4VP(BHBA)$_x$ samples.

For pristine BHBA, it is found that with different processing condition, different scattering result will be obtained. BHBA heated to 85 ℃ and cooled down slowly to ambient temperature (Fig. 4.3 (a) and (b), BHBA-Ann) shows typical diffraction of small molecule crystal with many sharp peaks in WAXS. By indexing diffraction peaks in WAXS with WinPLTOR and DICVOL software, a lattice cell with edges as a = 5.12 Å, b = 18.76 Å, c = 22.39 Å and angles as α = 90.48°, β = 90.82°, γ = 90.69° is obtained. By calculating the q-value of two diffraction peaks in SAXS, the d-spacing in larger scale of annealed BHBA is 22 Å and 17 Å, which is close to the result of WAXS.

On the other hand, BHBA heated to 85 ℃ and quenched into liquid nitrogen (Fig. 4.3 (a) and (b), BHBA-Que) performs differently than annealed BHBA. In WAXS (Fig. 4.3 (b)), the peaks is fewer and broader, inferring that BHBA aggregate is less ordered in BHBA-Que, and in SAXS, a periodic scattering peak in 1:2:3 ratio (0.123 Å^{-1}, 0.248 Å^{-1}, 0.370 Å^{-1}) is found and is believed to be a loose lamellar structure with repeating distance d = 51 Å as shown in Fig. 4.5. It is reasonable for quenched BHBA to performing larger d-spacing and less ordered structure, since the quenching froze the BHBA molecules in melt before the interdigitating and packing of BHBA tails occur.

For hydrogen-bonded comb-like supramolecules, unlike its three-tailed surfactant counterpart which forms hexagonally-packed cylinder structure, P4VP(BHBA)$_x$ does not result in any ordered structure in SAXS at any molar ratio x, but only perform a loose structure with d-spacing ~ 41 Å (q ~ 0.15 Å^{-1}), which is considered as the center-to-center

distance between P4VP(BHBA)$_x$ complexes. The assumption why ordered structure of hydrogen bonding does not appear in P4VP(BHBA)$_x$ complexes is that the volume of tails is neither suitable for lamellar and hexagonally-packed cylindrical structures. For lamellar structure, the volume of two tails is too large. On the other hand, the volume of two tails is not large enough for a complete hexagonally-packed cylindrical structures either. Therefore the structure of P4VP(BHBA)$_x$ complexes is considered as a disordered transition between lamella and hexagonally-packed cylinders.

Observed d-spacing about 41 Å is too short for end to end double layer structure (~ 60 Å). The explanation of d-spacing shorter than expected is assumed as the occurrence of interdigitating between BHBA domains in complexes. By inspecting the molecule model of BHBA (Fig. 4.6) drawn by Avogadro software, it is found that there is enough empty space between two tails of a BHBA molecule for inserting a carbon chain tail from another molecule. Also, the distance of interdigitating BHBA molecules binding with 4VP repeating unit evaluated by modeling software is 41.6 Å, which is agreed with observed d-spacing in SAXS. Note that the lamellar structure observed in scattering of BHBA-Que is also too short for end to end double layer structure, and therefore mild interdigitating is assumed (Figure 4.5).

For $x \leq 0.7$, with addition of BHBA, the d-spacing decreases due to extension of P4VP backbone by steric effect of hydrogen-bonding surfactants.[5] At the point of x = 0.8, the peak shifts to low q and broadens suddenly. This is considered as a trace amount of excess BHBA which is still not enough for aggregate by itself impairs the arrangement of P4VP(BHBA)$_x$ complexes by inserting into interdigitating layer of complexes, and therefore leads to larger d-spacing and worse uniformity. This inference also agrees with the above mentioned results of FTIR which show BHBA is excessive but unable to aggregate by itself.

In the interval of $0.9 \leq x \leq 1.0$, the peak of P4VP(BHBA)$_x$ complex structure recovers to larger d-spacing and narrower peak width the same as the one for $x = 0.7$, while the scattering peaks of aggregation of excess free BHBA, resembling the loose lamellar structure of BHBA after quench process (BHBA-Que in Fig. 4.3), is observed at $q = 0.266$ Å^{-1} in SAXS and $q = 1.47$ and 1.63 Å^{-1} in WAXS, indicating that excess BHBA aggregates into layer structure instead of inserting into interdigitating layer of P4VP(BHBA)$_x$ complex structure. Thus the complex structures are able to restore tighter packing and better order.

When x is higher than 1.2, shown in WAXS and high q range ($1.2 \sim 1.8$ Å^{-1}) of SAXS, scattering peaks resembling to annealed BHBA is detected, which indicates BHBA is able to crystallize with enough free surfactants. Also, the characteristic scattering peak of P4VP(BHBA)$_x$ complexes again shifts to lower q and become broader, inferring that complexes are more coiled and with less ordered packing, which agrees with the results of FTIR analysis. Therefore the detachment of BHBA from P4VA at high molar ratio is confirmed.

4.3 Thermal Behavior of P4VP(BHBA)$_x$

By using DSC, the thermal behavior of P4VP(BHBA)$_x$ can be studied. In Fig. 4.7 (a) and (b), for extensive investigate, all samples are investigated by DSC with the process of heating from 30 ℃ to 100 ℃ at the rate of 10 ℃/min, holding at 100 ℃ for 3 minutes and cooling from 100 ℃ to -40 ℃. In heating process (Fig. 4.7 (a)), for $x \leq 0.8$, no obvious melting peak can be found, which means that no free BHBA aggregates or crystals. For $0.9 \leq x \leq 1.0$, an exothermic peak (~ 60 ℃) is found below the melting peak of BHBA crystal (73 ~ 79 ℃), which is possibly the crystallization of excess BHBA aggregation. For $x \geq 1.2$, only melting peaks of BHBA is observed, implying that excess BHBA molecules all crystallize rather than aggregate into lamellar structure.

On the other hand, in cooling process (Fig. 4.7 (b)), a exothermic peak around 0 ℃ can be observed for all P4VP(BHBA)$_x$ samples, which is assigned to the crystallization peak of associated BHBA in P4VP(BHBA)$_x$ complexes. The crystallization temperature of BHBA in P4VP(BHBA)$_x$ complexes is far more lower than its three-tailed counterpart (THBA) in P4VP(THBA)$_x$ complexes (45 ℃) although the melting points of pure BHBA and THBA are nearly the same.[4] This suggests that the crystal structure of P4VP(BHBA)$_x$ complexes is far less stable than that of P4VP(THBA)$_x$.

From $x \leq 0.7$, the more the BHBA, the higher the crystallization temperature of BHBA in P4VP(BHBA)$_x$ complexes is. This is because higher concentration of BHBA and better alignment of complexes improve crystallization. When x comes to 0.8, the crystallization point of BHBA in complex drops for about 5 ℃, which is considered as the result of worse packing of P4VP(BHBA)$_x$ complexes with excess BHBA interruption. For $0.9 \leq x \leq 1.0$, the freezing points restored to higher temperature, indicating that excess BHBA aggregates into another phase rather than intercepts into P4VP(BHBA)$_x$

complexes, which is observed by SAXS and WAXS in former section. The crystallization point or melting points of pure BHBA aggregates is not found in P4VP(BHBA)$_{0.9\sim1.0}$, indicating that the aggregation of BHBA in these composition is not a typical crystal, but some other with less ordered structure, i.e. the lamellar structure in quenched BHBA, which is approved in former section. For $x \geq 1.2$, the crystallization points of pure BHBA crystal are observed and those of P4VP(BHBA)$_x$ complexes declines, in agreement with the crystallization and partial detachment of BHBA mentioned in above sections.

For better understanding about the thermal transition of P4VP(BHBA)$_x$ complexes, DSC at slower scanning rate (1 ℃/min) (Fig. 4.8) and in situ SAXS/WAXS (Fig. 4.8, Fig. 4.9 and Fig. 4.10) were applied on specific samples, which are x = 0.7 where the complexing is unsaturated, x = 0.9 where BHBA is excess and aggregates into lamellae???, and x = 1.4 for excess BHBA that crystallizes.

For x = 0.7, unlike Fig. 4.7 (a), weak exothermic and endothermic peaks are found with slower scanning rate at 60 and 70 ℃ respectively in Fig. 4.8 (a). These peaks are considered to be the realignment and melting of some relatively much ordered sites of BHBA in P4VP(BHBA)$_x$ complexes respectively, due to its higher melting temperature and low intensity of peaks. Realignment and melting are also recorded at 40 to 67 ℃ in Fig. 4.9 as the growth of the peak of P4VP(BHBA)$_x$ complex structure at 0.168 Å^{-1} in SAXS. While for x = 0.8, both recrystallization and melting is absent in Fig. 4.8 (a), which is resulted from the interference of excess BHBA among P4VP(BHBA)$_x$ complexes.

Then for x = 0.9, a massive recrystallizing peak is found around 40 ~ 60 ℃ in Fig. 4.8 (a). In Fig. 4.10 (b), it is found that peaks of the aggregation of BHBA intensify at 40 ~ 58 ℃ and transform into the peaks of BHBA crystal at 67 ~ 73 ℃. This is evident that the aggregation of excess BHBA transforms into BHBA crystal during heating scanning. On the other hand, the peak of P4VP(BHBA)$_x$ complex structure (~ 0.16 Å^{-1}) at first

increases at 40 ℃, then starts attenuating at 58 ℃ and finally disappears at 67 ℃ in Fig. 4.10 (a), which can be interpreted as recrystallizing, and detachment of P4VP(BHBA)$_x$ complexes due to competition from excess BHBA crystallization.[4]

Last for x = 1.4, in Fig. 4.9 (a), it is shown that the diffraction peaks of BHBA crystal exists from the most beginning, and changes into different pattern at 67 ℃, suggesting that transition of different type of crystal occurs, which is also confirmed by two melting points (66 ℃ and 76 ℃). As well, the attenuation of the peak of P4VP(BHBA)$_x$ complex structure (~ 0.16 Å $^{-1}$) is considered because of competition of BHBA crystals.[4]

By summarizing FTIR, DSC, SAXS and WAXS analysis mentioned above, the evolution of P4VP(BHBA)$_x$ complex system is concluded into following four regimes like Fig. 4.12

1. $0 \leq x \leq 0.7$: P4VP(BHBA)$_x$ complex forms a loose structure with d ~ 41Å with BHBA mildly interdigitated.
2. x = 0.8: excess BHBA interact with BHBA attached on P4VP, leading to looser structure with larger d (~ 46Å).
3. $0.9 \leq x \leq 1.0$: excess BHBA aggregates into the lamellar structure similar to the one after quenched, while leaving P4VP(BHBA)$_x$ complex the same as section 1.
4. $1.2 \leq x$: excess BHBA crystallizes into crystal. Partial detachment of BHBA from P4VP occurs, resulting in coiling of P4VP and looser structure with larger d (~ 46Å).

As BHBA contains only two tails, P4VP(BHBA)$_x$ complex performs unique properties that are absent in systems with one or three-tailed surfactants. No ordered structure forms but only a repeating spacing is observed in all x range, due to the volume of tail domain is neither favorable for lamellar nor hexagonally-packed cylindrical

structure. This also induces a low crystallization point of hydrogen bonded BHBA around 0 ℃. With the space between two legs, interdigitating is allowed in BHBA domain of P4VP(BHBA)$_x$ complexes, or excess BHBA aggregates before crystallization begins.

As molar ratio *x* of BHBA to 4VP reaches 0.8, which is just slightly higher than saturation, excess BHBA interferes the alignment of P4VP(BHBA)$_x$ complexes and leads to much disordered structure by inserting into interdigitating in BHBA domain. As BHBA increases, lamellar aggregation forms instead of interrupting P4VP(BHBA)$_x$ complexes interaction, and therefore alignment of complexes restores. For BHBA is abundant enough for crystallization, the competition between crystallization and hydrogen bonding is observed as others reported.[4]

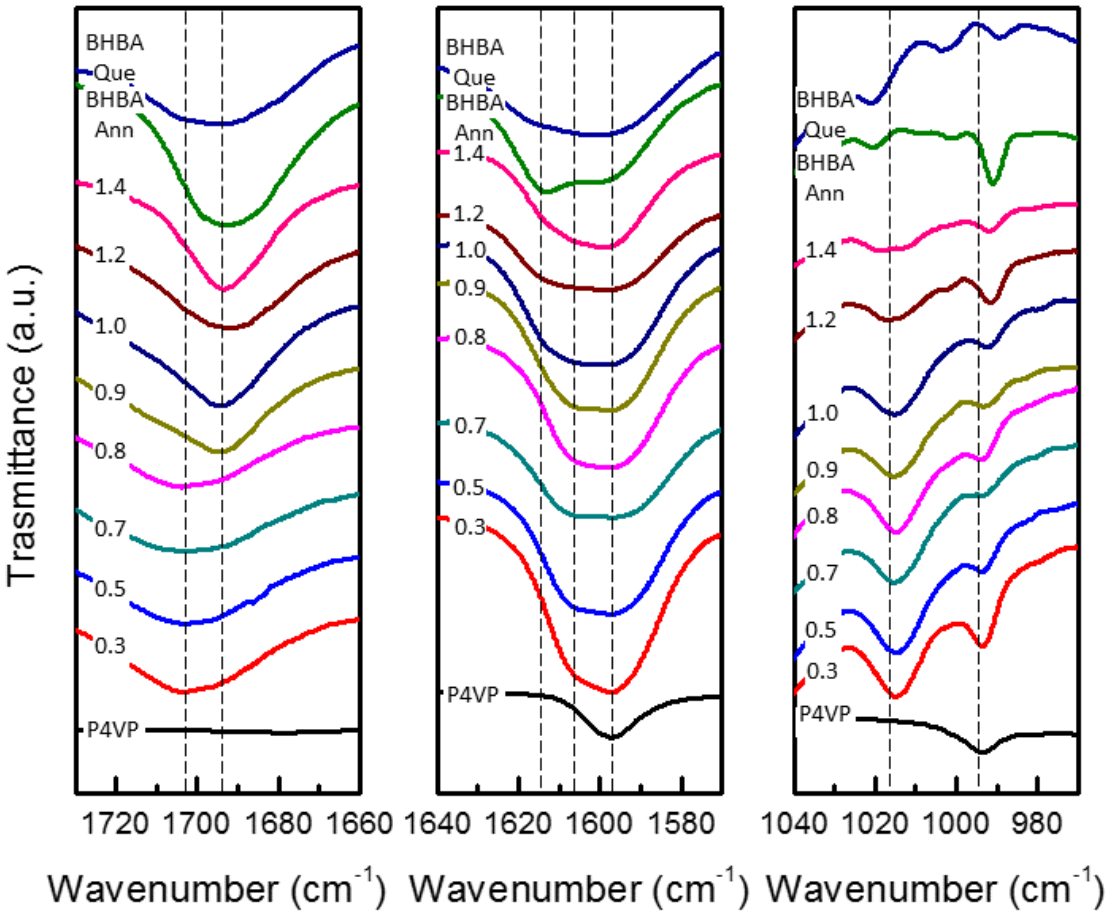

Figure. 4.1 FTIR spectra of the P4VP, P4VP(BHBA)$_x$ and BHBA samples, where the numbers are the molar ratio x of P4VP(BHBA)$_x$ samples, and BHBA Ann and BHBA Que are BHBA after annealing process and quench process respectively.

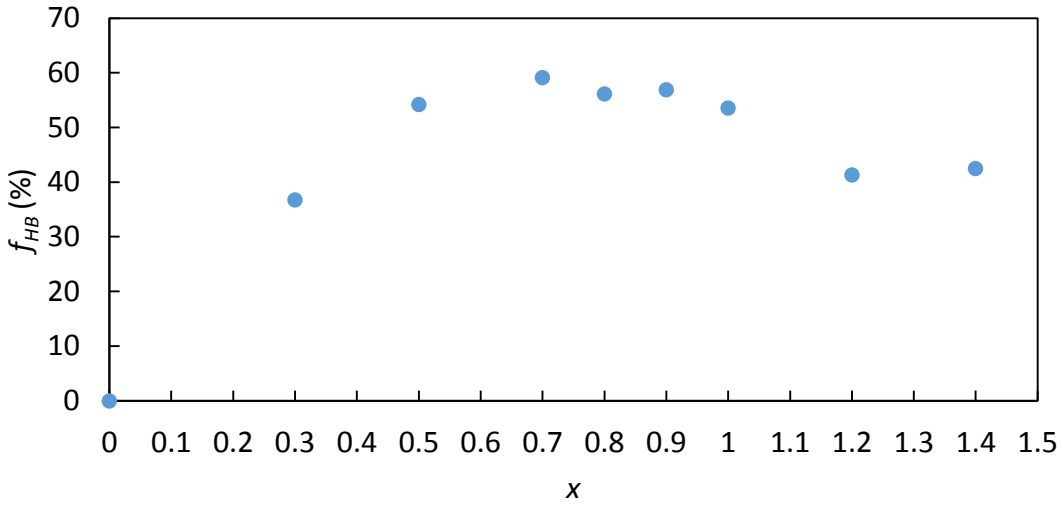

Figure. 4.2 Degrees of grafting (f_{HB}) of P4VP(BHBA)$_x$ samples

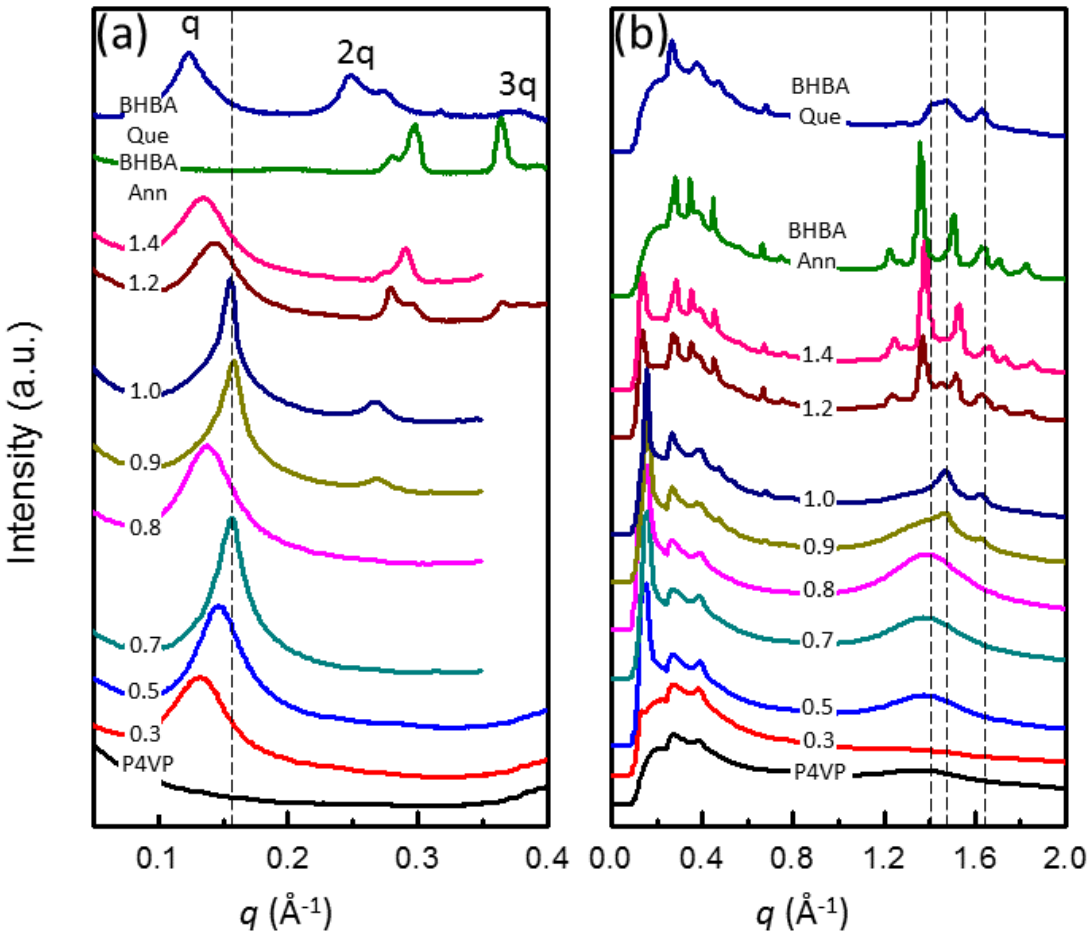

Figure. 4.3 (a) SAXS and (b) WAXS intensity profiles of P4VP, P4VP(BHBA)$_x$ and BHBA samples, where the numbers are the molar ratio x of P4VP(BHBA)$_x$ samples, and BHBA Ann and BHBA Que are BHBA after annealing process and quench process respectively.

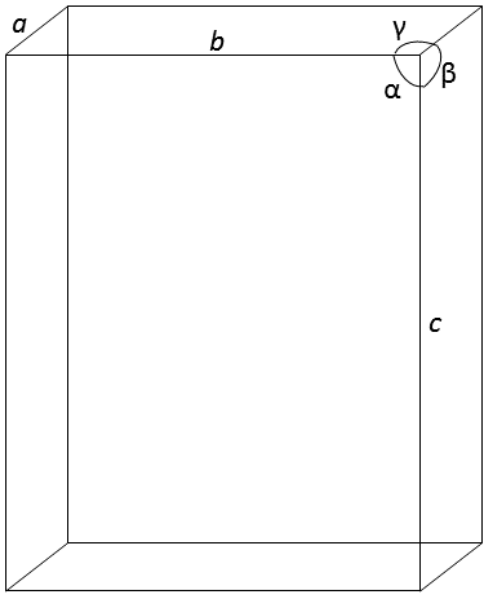

Figure 4.4 The lattice cell of annealed BHBA, where cell edges are a = 5.12 Å , b = 18.76 Å , c = 22.39 Å and angles are α = 90.48°, β = 90.82°, γ = 90.69°.

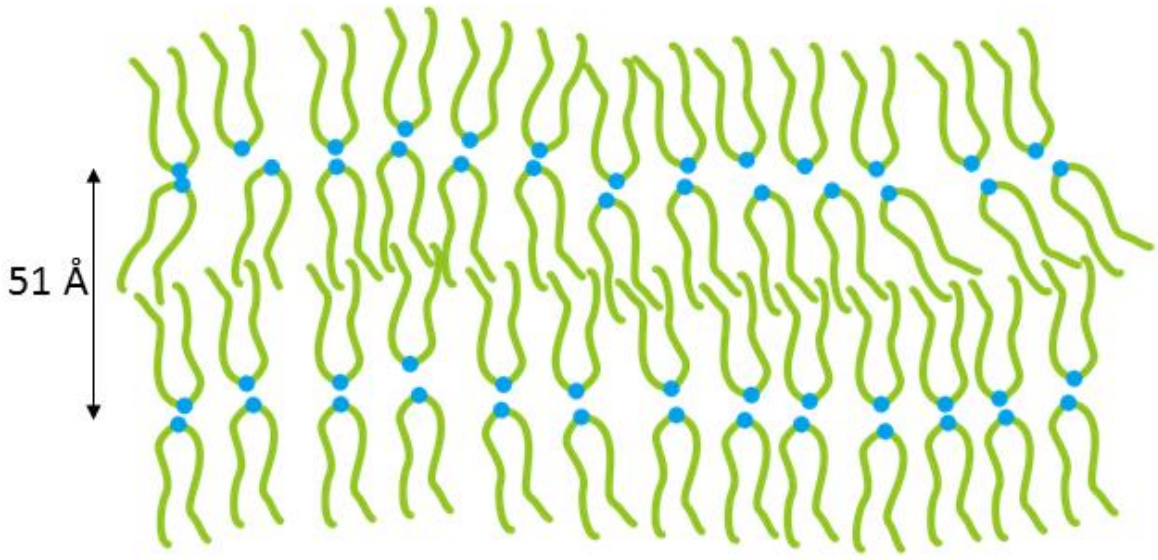

Figure 4.5 The structure of quenched BHBA, where blue circles are head group of BHBA and green lines are tails of BHBA

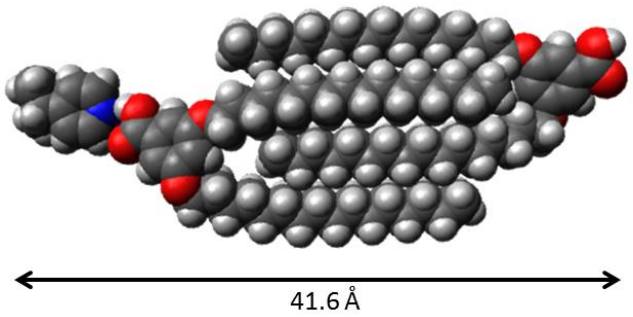

Figure 4.6 The van der Waals ball model of two interdigitating BHBA binding on a 4VP repeating unit.

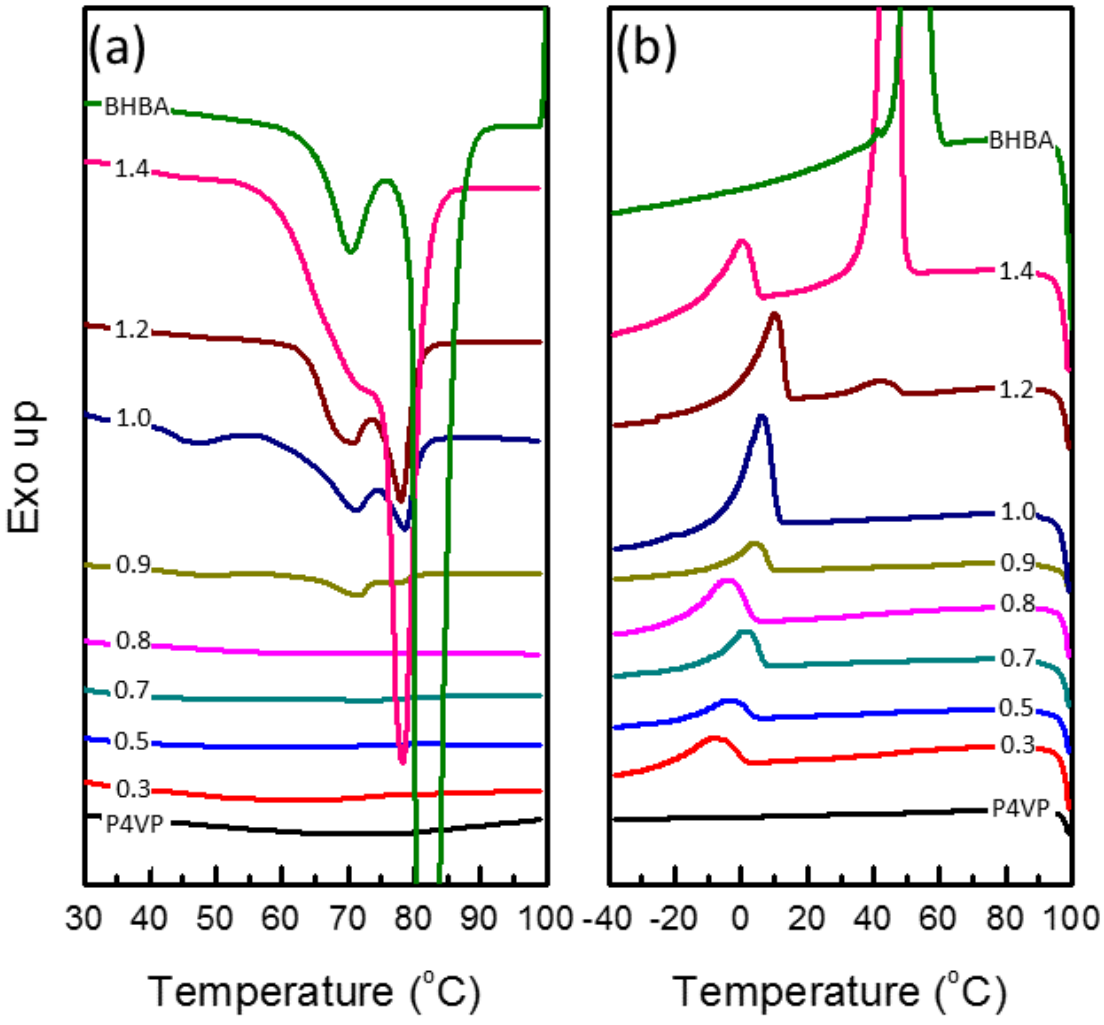

Figure 4.7 Heat profiles of P4VP(BHBA)$_x$ samples, where the conditions of DSC are (a) heating from 30 ℃ to 100 ℃ at 10 ℃/min and (b) cooling from 100 ℃ to -40 ℃ at 10 ℃/min.

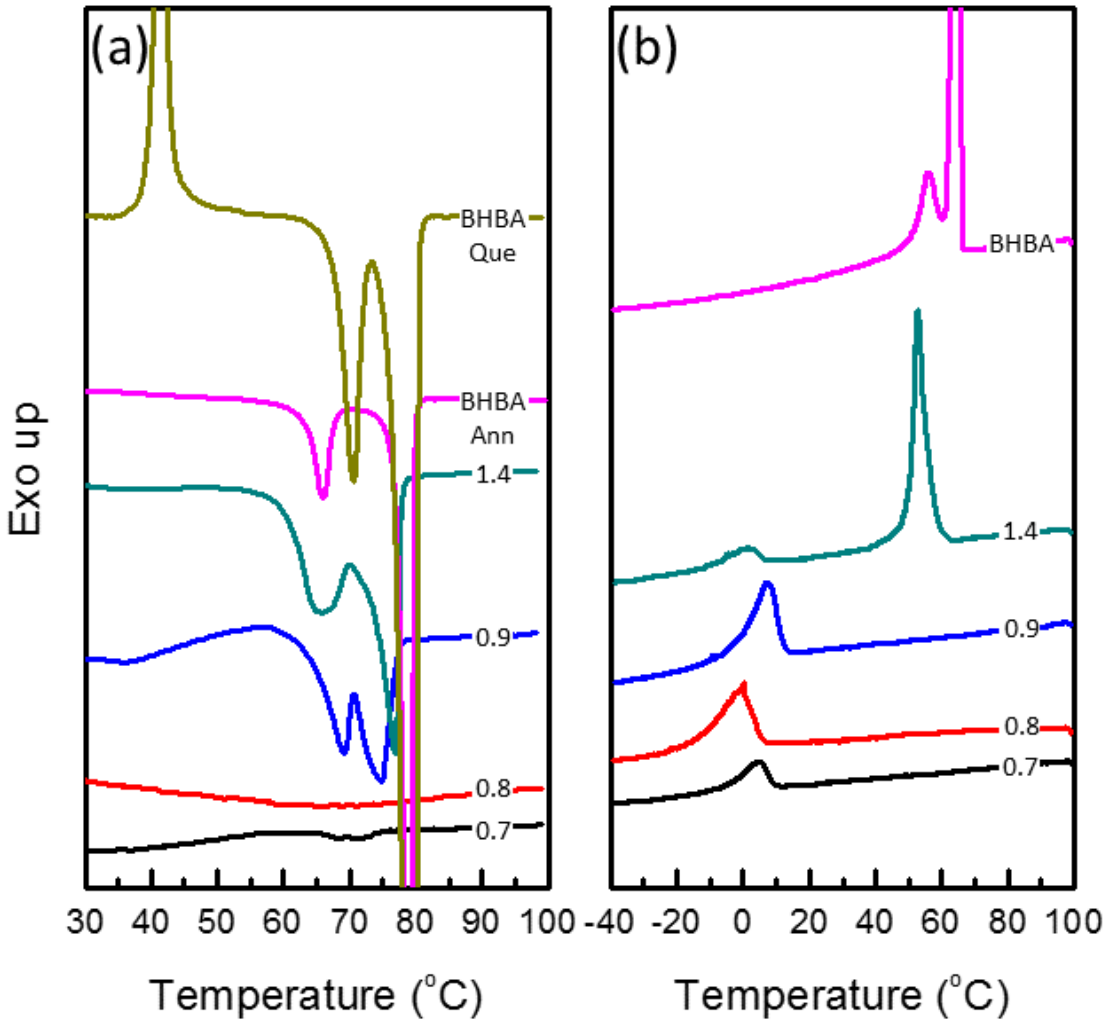

Figure 4.8 Heat profiles of P4VP(BHBA)$_x$ samples, where the conditions of DSC are (a) heating from 30 ℃ to 100 ℃ at 1 ℃/min and (b) cooling from 100 ℃ to 30 ℃ at 1 ℃/min.

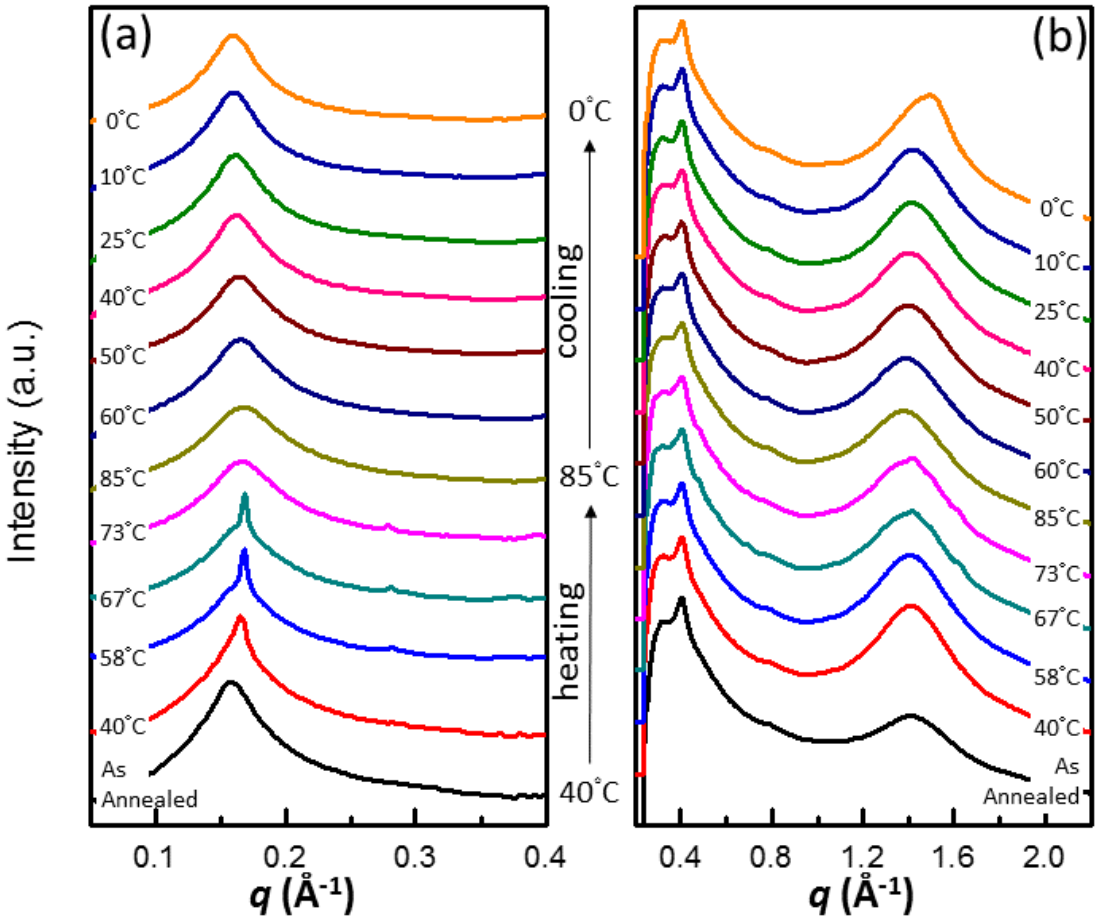

Figure 4.9 (a) SAXS and (b) WAXS profiles of P4VP(BHBA)$_{0.7}$ at different temperatures.

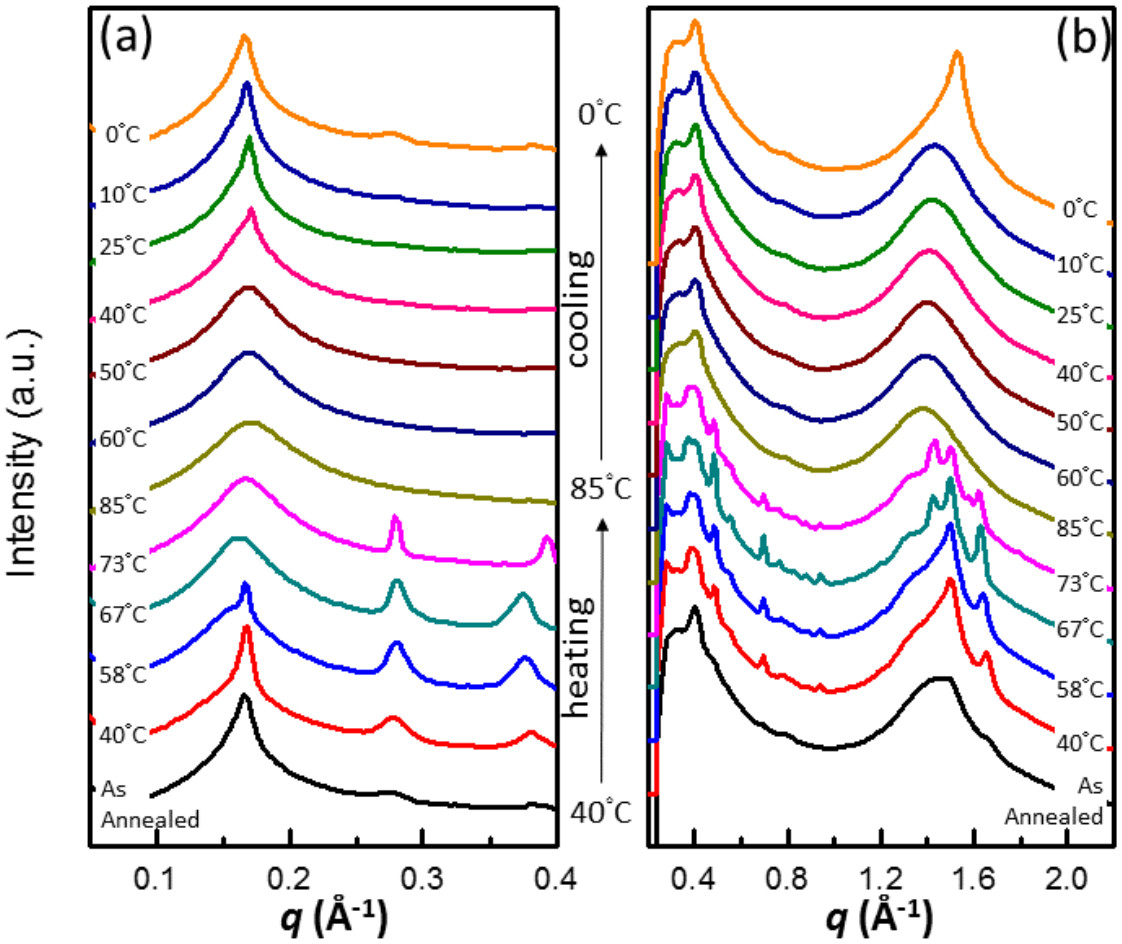

Figure 4.10 (a) SAXS and (b) WAXS profiles of P4VP(BHBA)$_{0.9}$ at different temperatures.

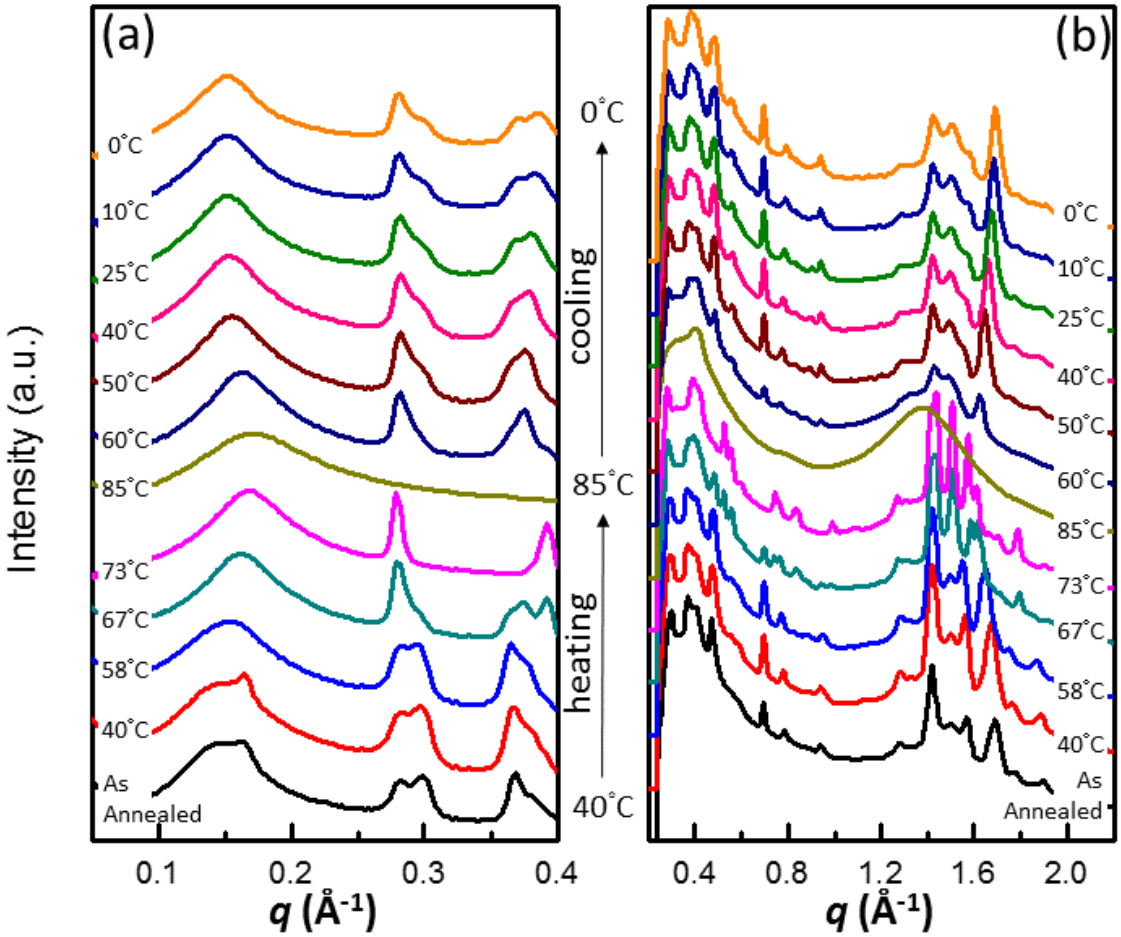

Figure 4.11 (a) SAXS and (b) WAXS profiles of P4VP(BHBA)$_{1.4}$ at different temperatures.

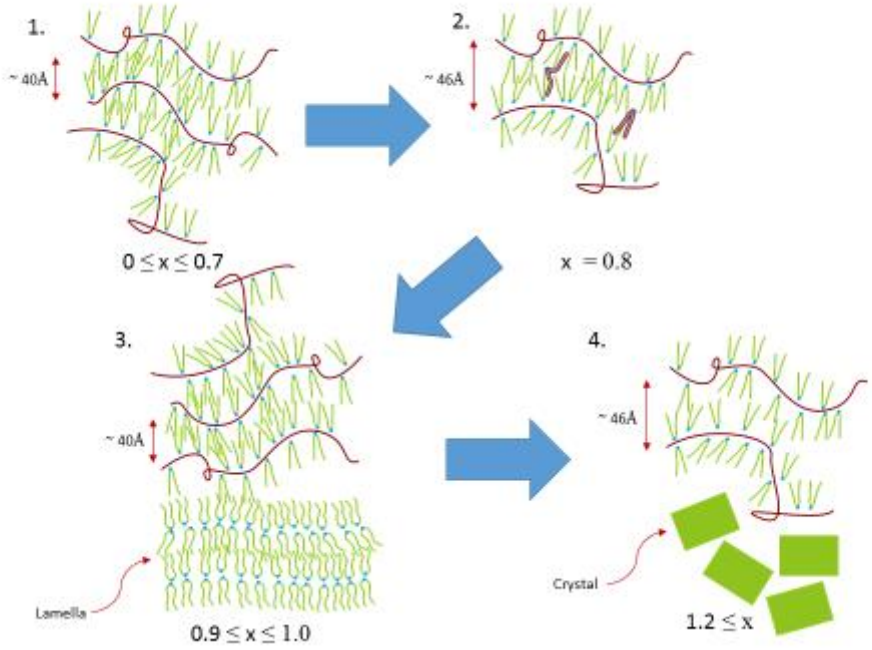

Figure 4.12 The cartoon about sections of P4VP(BHBA)$_x$ complex system with different molar ratio *x*, while purple lines are P4VP backbone, blue circles are head group of BHBA, green lines are tails of BHBA and green slabs are crystals of BHBA.

Chapter 5 Conclusion

In this study, as the untouched part of past studied about hydrogen-bonded comb-like system, the property of hydrogen-bonded comb-like system with surfactant with two tails has been investigated. It is interesting to find that a hydrogen-bonded comb-like system with surfactant with two tails performs totally different from those with single tails or three tails. With steric hindrance of tails neither suitable for lamella nor hexagonally-packing cylinders, P4VP(BHBA)$_x$ complex performs no highly ordered structure at any molar ratio x of BHBA and at any temperature. Furthermore, the absence of middle tail provides enough free space for interdigitating between BHBA molecules, and therefore makes it possible that excess BHBA can interfere the alignment of P4VP(BHBA)$_x$ complexes drastically at x = 0.8, by inserting into the free space which is for interdigitating between BHBA domains in P4VP(BHBA)$_x$ complexes. Overall the systems of hydrogen-bonded comb-like system with two-tailed surfactant performs less ordered than one with three-tailed surfactant.

Low melting point and less ordered structure of P4VP(BHBA)$_x$ complex are potential for application in rheological study in ambient temperature.[25] Also, in this research, only 3,5-bis substituted surfactant is applied. As single-tailed surfactants with different substitution sites will perform differently in hydrogen-bonded comb-like supramolecular system[26], the study of 3,4-bis substituted surfactant, if the problem of solubility can be solved, is expected to show some other interesting result.

REFERENCE

1. Lehn, J.M., *SUPRAMOLECULAR CHEMISTRY - SCOPE AND PERSPECTIVES MOLECULES, SUPERMOLECULES, AND MOLECULAR DEVICES.* Angewandte Chemie-International Edition in English, 1988. **27**(1): p. 89-112.
2. ten Brinke, G., J. Ruokolainen, and O. Ikkala, *Supramolecular materials based on hydrogen-bonded polymers*, in *Hydrogen Bonded Polymers*, W. Binder, Editor. 2007, Springer-Verlag Berlin: Berlin. p. 113-177.
3. Pollino, J.M. and M. Weck, *Non-covalent side-chain polymers: design principles, functionalization strategies, and perspectives.* Chemical Society Reviews, 2005. **34**(3): p. 193-207.
4. Lai, T.-Y., et al., *Phase Behavior and Structure of Supramolecules Formed by Poly(4-vinylpyridine) and Fanlike Benzoic Acid Derivative with Long Hydrophobic Tails.* Macromolecules, 2015. **48**(3): p. 717-724.
5. Wang, S.-J., et al., *Phase Behavior of a Hydrogen-Bonded Polymer with Lamella-to-Cylinder Transition: Complex of Poly(4-vinylpyridine) and Small Dendritic Benzoic Acid Derivative.* Macromolecules, 2012. **45**(21): p. 8760-8769.
6. Chuang, W.-T., et al., *Tetragonally Perforated Layer Structure via Columnar Ordering of 4´-(3,4,5-Trioctyloxybenzoyloxy)benzoic Acid in a Supramolecular Complex with Polystyrene-block-Poly(4-vinylpyridine).* Chemistry of Materials, 2009. **21**(6): p. 975-978.
7. Chuang, W.-T., et al., *Directing the Interfacial Morphology of Hierarchical Structures of Dendron-Jacketed Block Copolymers via Liquid Crystalline Phases.* Macromolecules, 2014. **47**(17): p. 6047-6054.
8. Zhu, X., et al., *Self-Organization of Polybases Neutralized with Mesogenic Wedge-Shaped Sulfonic Acid Molecules: An Approach toward Supramolecular Cylinders.* Journal of the American Chemical Society, 2006. **128**(51): p. 16928-16937.
9. Liu, X., et al., *Hydrogen-Bonded Polymers with Bent-Shaped Side Chains and Poly(4-vinylpridine) Backbone: Phase Behavior and Thin Film Morphologies.* Macromolecules, 2014. **47**(12): p. 3917-3925.
10. Wang, S.-J., et al., *A complex of poly(4-vinylpyridine) and tolane based hemi-phasmid benzoic acid: towards luminescent supramolecular side-chain liquid crystalline polymers.* Chemical Communications, 2014. **50**(61): p. 8378-8381.
11. Ruokolainen, J., et al., *Mesomorphic Structures in Flexible Polymer−Surfactant Systems Due to Hydrogen Bonding: Poly(4-vinylpyridine)−Pentadecylphenol.* Macromolecules, 1996. **29**(10): p. 3409-3415.
12. Ikkala, O., et al., *Ordering in self-organizing comb copolymer-like systems obtained by hydrogen bonding between charged or noncharged polymers and amphiphiles.* Colloids and Surfaces A: Physicochemical and Engineering Aspects, 1999. **147**(1–2): p. 241-248.
13. Ikkala, O., et al., *Surfactant induced mesomorphic behaviour of flexible polymers.* Macromolecular Symposia, 1996. **112**(1): p. 191-198.
14. Ruokolainen, J., et al., *Direct Imaging of Self-Organized Comb Copolymer-like Systems Obtained by Hydrogen Bonding: Poly(4-vinylpyridine)−4-Nonadecylphenol.* Macromolecules, 1998. **31**(11): p. 3532-3536.
15. Chao, C.Y., et al., *Orientational Switching of Mesogens and Microdomains in Hydrogen-Bonded Side-Chain Liquid-Crystalline Block Copolymers Using AC*

Electric Fields. Advanced Functional Materials, 2004. **14**(4): p. 364-370.
16. Kosonen, H., et al., *Self-organized supermolecules based on conducting polyaniline and hydrogen bonded amphiphiles.* Synthetic Metals, 2001. **121**(1–3): p. 1277-1278.
17. Kosonen, H., et al., *Nanoscale conducting cylinders based on self-organization of hydrogen-bonded polyaniline supramolecules.* Macromolecules, 2000. **33**(23): p. 8671-8675.
18. Ikkala, O. and G. ten Brinke, *Functional Materials Based on Self-Assembly of Polymeric Supramolecules.* Science, 2002. **295**(5564): p. 2407-2409.
19. Ikkala, O. and G. ten Brinke, *Hierarchical self-assembly in polymeric complexes: Towards functional materials.* Chemical Communications, 2004(19): p. 2131-2137.
20. Ruokolainen, J., et al., *Critical Interaction Strength for Surfactant-Induced Mesomorphic Structures in Polymer−Surfactant Systems.* Macromolecules, 1996. **29**(20): p. 6621-6628.
21. Korhonen, J.T., et al., *Self-Assembly and Hierarchies in Pyridine-Containing Homopolymers and Block Copolymers with Hydrogen-Bonded Cholesteric Side-Chains.* Macromolecules, 2010. **43**(3): p. 1507-1514.
22. Millikan, R.C. and K.S. Pitzer, *The Infrared Spectra of Dimeric and Crystalline Formic Acid.* Journal of the American Chemical Society, 1958. **80**(14): p. 3515-3521.
23. Lee, J.Y., P.C. Painter, and M.M. Coleman, *Hydrogen bonding in polymer blends. 4. Blends involving polymers containing methacrylic acid and vinylpyridine groups.* Macromolecules, 1988. **21**(4): p. 954-960.
24. Luyten, M.C., et al., *Crystallization and Cocrystallization in Supramolecular Comb Copolymer-like Systems: Blends of Poly(4-vinylpyridine) and Pentadecylphenol.* Macromolecules, 1999. **32**(13): p. 4404-4410.
25. de Moel, K., et al., *Oscillatory Shear Flow-Induced Alignment of Lamellar Melts of Hydrogen-Bonded Comb Copolymer Supramolecules.* Macromolecules, 2001. **34**(9): p. 2892-2900.
26. Hofman, A.H., et al., *Interaction Strength in Poly(4-vinylpyridine)–n-Alkylphenol Supramolecular Comb-Shaped Copolymers.* Macromolecules, 2015. **48**(5): p. 1554-1562.